Photolabile Precursors of Biological Amides: Synthesis and Characterization of Caged *o*-Nitrobenzyl Derivatives of Glutamine, Asparagine, Glycinamide, and γ-Aminobutyramide

Doraiswamy Ramesh, Raymond Wieboldt, Andrew P. Billington, Barry K. Carpenter,† and George P. Hess*

Section of Biochemistry, Molecular and Cell Biology, Division of Biological Sciences, 217 Biotechnology Building, Cornell University, Ithaca, New York 14853-2703

Received December 30, 1992

The synthesis and photochemical properties of *o*-nitrobenzyl derivatives of glutamine, asparagine, glycinamide, and γ-aminobutyramide (GABA amide) linked through the amide nitrogen are reported. The time scale for the release of the amides from the photolabile *o*-nitrobenzyl protecting group was unknown and has now been investigated. The compounds are photolyzed by UV irradiation at 308 and 350 nm to release free amino acid amide and the presumed aromatic nitroso side product, with quantum yields in the range of 0.13 for the methyl derivative of glutamine (**20**) to 0.24 for the carboxy derivative of glutamine (**21**). Both pH and the α-substituent of the *o*-nitrobenzyl protecting group affect the rate of the photolysis reaction, which is initiated by a single laser pulse at 308 nm and monitored by the optical absorbance decay time course of the transient *aci*-nitro anion intermediate. The rate of disappearance of this intermediate, assumed to reflect the appearance of products, is influenced by pH and the α-substituent attached to the benzylic carbon. For example, the rates for the α-carboxyl (**21**) and α-H (**19**) derivatives of glutamine increase by a factor of 50 as the pH is lowered from 11.5 to 5.5, whereas the rate for the α-methyl derivative (**20**) shows a minimum at pH 9.5. The half lives of the *aci*-nitro intermediates of the α-methyl, α-carboxyl, and α-H derivatives of glutamine at pH 7.5 are 360, 720, and 1800 μs, respectively.

Rapid release of biologically active molecules from photolabile precursors is gaining increased application in the study of fast kinetic processes of biological significance that are not easily accessible by other biophysical methods. The design and applications of these "caged compounds"[1] have been reviewed.[2a–d] Photoreleasable substrates have found application in biophysical research in such areas as ATP-induced muscle contraction,[3] the role of calcium in intracellular signal transduction pathways,[4a–d] and activation of second messenger systems by photolytic release of inositol trisphosphates.[5] Photolabile precursors have been used in time-resolved X-ray crystallography studies to determine ligand-induced conformational changes, which are observed in the crystal structure of GTP-binding proteins and which occur after photolytic release of the free substrate inside the crystal lattice.[6] The caged compound strategy has also been used for aminoacylation of transfer RNAs[7] and in novel self-replicating molecular systems.[8] Caged compounds provide unprecedented spatial[9] and temporal[10] control of ligand concentration in systems where diffusional mixing delays are a barrier to observation of rapid kinetic events. For example, the rapid release of a caged neurotransmitter was used to determine rate constants in the mechanism of the fast channel-opening process in neuronal receptors.[10,11] The *o*-nitroveratryl derivatives[12] of amino acids and the *o*-nitrobenzyl derivatives of carbamoylcholine[13] and glycine[14] have been shown to release free neurotransmitter, which activates ion-channel receptors on a millisecond time scale. The photolytic release of carbamoylcholine was faster than the opening of the nicotinic acetylcholine receptor-channel in the BC_3H1 cell line, and the laser-pulse photolysis technique has been used to determine the rate constant for the formation of the transmembrane channel.[10]

Biological amides play an important role in plant and animal nitrogen metabolism[15] and in many other biochemical and physiological mechanisms. The caged amide linkage reported here is applicable to derivatization of urea, and a photolabile derivative of urea could be useful in structural and kinetic studies of the enzyme urease. Glutamine and asparagine participate in many metabolic functions that have been studied for both biochemical

* Address all correspondence to this author.
† Department of Chemistry, Cornell University, Ithaca, NY 14853.

(1) Kaplan, J. H.; Forbush, B.; Hoffman, J. F. *Biochemistry* **1978**, *17*, 1929.
(2) (a) McCray, J. A.; Trentham, D. R. *Annu. Rev. Biophys. Biophys. Chem.* **1989**, *18*, 239. (b) Kaplan, J. H.; Somlyo, A. P. *Trends Neurosci.* **1989**, *12*, 54. (c) Kaplan, J. H. *Ann. Rev. Physiol.* **1990**, *52*, 897. (d) Adams, S. R.; Tsien, R. Y. *Ann. Rev. Physiol.* **1993**, *55*, 755.
(3) Gurney, A. M.; Lester, H. A. *Physiol. Rev.* **1987**, *67*, 583.
(4) (a) Kaplan, J. H.; Ellis-Davies, G. C. R. *Proc. Nat. Acad. Sci. U.S.A.* **1988**, *85*, 6571. (b) Ellis-Davies, G. C. R.; Kaplan, J. H. *J. Org. Chem.* **1988**, *53*, 1966. (c) Adams, S. R.; Kao, J. P. Y.; Grynkiewicz, G.; Minta, A.; Tsien, R. Y. *J. Am. Chem. Soc.* **1988**, *110*, 3212. (d) Kao, J. P. Y.; Harootunian, A. T.; Tsien, R. Y. *J. Biol. Chem.* **1989**, *264*, 8179.
(5) (a) Blatt, M. R.; Theil, G.; Trentham, D. R. *Nature* **1990**, *346*, 766. (b) Gilroy, S.; Read, N. D.; Trewavas, A. J. *Nature* **1990**, *346*, 769.
(6) Schlichting, I.; Almo, S. C.; Rapp, G.; Wilson, K.; Petratos, K.; Lentfer, A.; Wittinghofer, A.; Kabsch, W.; Pai, E. F.; Petsko, G. A.; Goody, R. S. *Nature* **1990**, *345*, 309.
(7) Robertson, S. A.; Ellman, J. A.; Schultz, P. G. *J. Am. Chem. Soc.* **1991**, *113*, 2722.
(8) Hong, J.-I.; Feng, Q.; Rotello, V.; Rebek, J. *Science* **1992**, *255*, 848.
(9) Fodor, S. P. A.; Read, J. L.; Pirrung, M. C.; Stryer, L.; Lu, A. T.; Solas, D. *Science* **1991**, *251*, 767.
(10) Matsubara, N.; Billington, A. P.; Hess, G. P. *Biochemistry* **1992**, *31*, 5477.
(11) Niu, L.; Hess, G. P. *Biochemistry* **1993**, *32*, 3831.
(12) Wilcox, M.; Viola, R. W.; Johnson, K. W.; Billington, A. P.; Carpenter, B. K.; McCray, J. A.; Guzikowski, A. P.; Hess, G. P. *J. Org. Chem.* **1990**, *55*, 1585.
(13) (a) Walker, J. W.; McCray, J. A.; Hess, G. P. *Biochemistry* **1986**, *25*, 1799. (b) Milburn, T.; Matsubara, N.; Billington, A. P.; Udgaonkar, J. B.; Walker, J. W.; Carpenter, B. K.; Webb, W. W.; Marque, J.; Denk, W.; McCray, J. A.; Hess, G. P. *Biochemistry* **1989**, *28*, 49.
(14) Billington, A. P.; Walstrom, K. M.; Ramesh, D.; Guzikowski, A. P.; Carpenter, B. K.; Hess, G. P. *Biochemistry* **1992**, *31*, 5500.
(15) (a) Harms, E.; Wehner, A.; Aung, H.-P.; Roehm, K. H. *FEBS Lett.* **1991**, *285*, 55. (b) Frankenberger, W. T.; Tabatabai, M. A. *Biol. Fertil. Soils* **1991**, *11*, 6.

0022-3263/93/1958-4599$04.00/0

and therapeutic reasons. For example, asparaginase (L-asparagine amidohydrolase EC 3.5.1.1) catalyzes the hydrolysis of asparagine to aspartate and is an effective agent in the treatment of lymphoblastic leukemia.[16] Crystal structures of the enzyme are available, but the mechanistic details of the binding and catalytic steps are not fully understood.[17] Another important physiological role of asparagine is associated with the inhibition of brain asparaginase by opiates.[18] This interaction is hypothesized to be the main factor in physical opioid dependence. In metabolic studies, glutamine has been shown to induce membrane depolarization in developing soybean embryos.[19] The details of the underlying transport mechanisms are unclear,[20] but are known to have an important effect on seed yield and nutritional quality.

We report here the synthesis and photochemical characterization of seven photolabile precursors of amino acid amides, asparagine, glutamine, γ-aminobutyramide, and glycinamide. The time region in which the amides are released from the photolabile *o*-nitrobenzyl protecting group is also reported. The method is generally applicable to systems where photoproduction of free amides is desired and complements reported methods of photolytic production of amides[21] and release of amides bound to solid matrices.[22a-d] The compounds were shown to release the free amino acid amides rapidly as a result of photolysis with a pulsed UV laser light source. The photolysis rate and yield of the compounds in aqueous buffer at room temperature were investigated using conventional laser-pulse photolysis and HPLC.

Results and Discussion

The synthetic procedure for the caged amides **15-21** forms the photolabile amino acid amide from a primary amine (**1**, **2**, or **3**) and carboxylic acids **I** or **II**. Compounds represented by **I** are amine-protected amino acids and by **II** are both amine- and carboxy-protected carboxylic amino acids. A single reaction pathway was required to synthesize the seven caged amides with the 2-nitrobenzyl protecting group (Scheme I, **15-21**). The first step involves the formation of an amide bond between the amine of the photolabile group of **1**, **2**, or **3** and the unprotected carboxylic acid group on the *N*-t-Boc and t-Boc protected amino-acid derivatives **4-7**. The reaction in the presence of DMAP, NEM, NHBT, and EDCI was allowed to proceed for 12 h and found to yield the protected photolabile molecules **8-14**. Acid deprotection then produced the photolabile amide precursors. The general procedure employs conditions that minimize racemization of the amino acid during the coupling and deprotection steps[23] and provides a simple, high-yield route to the protected amides.

Scheme I

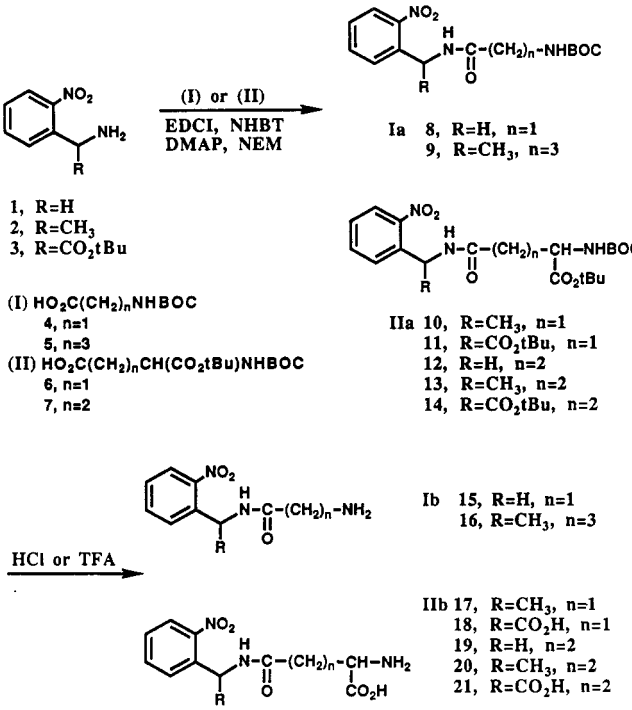

The photochemical reaction of *o*-nitrobenzyl compounds has been reviewed.[24] In general, photorelease of the leaving group (in this case, amino acid amide) is accompanied by the production of a nitroso side product that is responsible for the characteristic spectral behavior observed with this class of compounds.[25] Photolysis of the caged amides by pulsed laser irradiation at 308 nm produced changes in the UV-vis spectra typified by the the traces shown in Figure 1a for compound **21**. Each compound investigated exhibited a characteristic spectrum at pH 7.4 of the *o*-nitrobenzyl system of the unphotolyzed material with an absorption maximum near 270 nm. Photolysis produced an increase in the absorbance at 330 and 240 nm. Compounds **15**, **18**, **19**, and **21** showed clear isosbestic points for the initial conversion from starting material to product, followed by a small but progressive deviation as the extent of conversion reached 100%. Compounds **16**, **17**, and **20**, however, exhibited larger deviations during photolysis and did not produce isosbestic points, even in the initial stages of the photolysis reaction.

The caged amides synthesized also release amino acid amides when irradiated with 350-nm light in a Rayonet photochemical reactor. The release of both free amino acid amides and the presumed *o*-nitrosophenyl side product was confirmed by HPLC. Fluorescence monitoring was used to observe released amino amides derivatized with OPA (see Experimental Section), whereas both the *o*-nitrobenzyl and the aromatic side product were detected using absorbance monitoring at wavelengths between 240 and 280 nm. Figure 1b gives an example of the separation of the photolysis reaction products using both detection methods. For qualitative identification of the reaction components, photolysis conditions were chosen such that 1-5% of the starting material was converted to products. Photolysis was performed on 5 μL of solution in a 100-μm borosilicate melting point capillary,

(16) Capizzi, R. L.; Cheng, Y. In *Enzymes as Drugs*; Holcenberg, J. S., Robert, J., Eds.; Wiley: New York; 1981.
(17) (a) Dunlop, P. C.; Mayer, G. M.; Roon, R. J. *J. Biol. Chem.* **1980**, *255*, 1542. (b) Wriston, J. R. In *Methods of Enzymology*; Meister, A., Ed.; Academic Press: New York, 1985; Vol. 113, p 608.
(18) Koyuncuoglu, H.; Gungor, M.; Sagduyu, H.; Aricioglu, F. *Pharmacol. Biochem. Behav.* **1990**, *35*, 829.
(19) Bennett, A. B.; Spanswick, R. M. *Physiol. Plant* **1983**, *72*, 781.
(20) Peeters, K. M. U.; van Laere, A. J. *Physiol. Plant* **1992**, *84*, 243.
(21) Henriksen, D. B.; Breddam, K.; Møller, J.; Buchardt, O. *J. Am. Chem. Soc.* **1992**, *114*, 1876.
(22) (a) Rich, D. H.; Gurwara, S. K. *Tetrahedron Lett.* **1975**, 301. (b) Pillai, V. N. R.; Mutter, M.; Bayer, E. *Tetrahedron Lett.* **1979**, 3409. (c) Pillai, V. N. R. *Synthesis* **1980**, *1*, 1. (d) Ajayaghosh, A.; Pillai, V. N. R. *Ind. J. Chem.* **1988**, *27B*, 1004. (e) Ajayaghosh, A.; Pillai, V. N. R. *J. Org. Chem.* **1990**, *55*, 2826.
(23) König, W.; Geiger, R. *Chem. Ber.* **1970**, *103*, 788.
(24) Chow, Y. L. In *The Chemistry of Amino, Nitroso and Nitro Compounds and Their Derivatives*; Patai, S., Ed.; New York: Wiley & Sons; 1982; p 181.
(25) Peyser, J. R.; Flechtner, T. W. *J. Org. Chem.* **1987**, *52*, 4645.

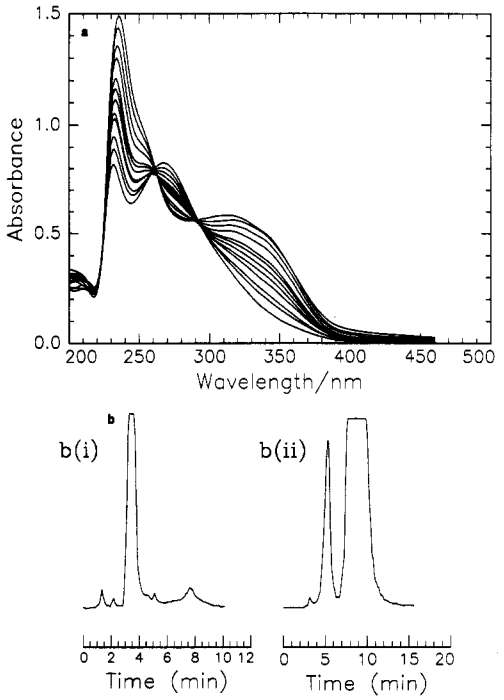

Figure 1. (a) UV–vis spectrum of the photolysis reaction of compound **21**. 35 μL of 2 mM solution of **21** in 200 mM HEPES buffer, pH 7.4, was photolyzed with 308-nm light from an excimer laser in a 2- × 2-mm cuvet. The lowest trace at 340 nm is the spectrum of unphotolyzed starting material, followed by spectra taken after 1, 2, 3, 4, 6, 8, 10, 15, 20, 30, and 50 laser pulses. (b) Reversed-phase HPLC separation of photolyzed **21**. Absorbance detection at the reaction isosbestic point (263 nm) was used in i; fluorescence detection was used in ii. The unphotolyzed caged glutamine signal is offscale in i at a retention time of 3.1 min. Photolysis produces a signal at 7.7 min, corresponding to the presumed aromatic nitroso keto acid side product. In ii the fluorescently labeled glutamine produced by photolysis elutes at 5.2 min. The offscale peak at 10.0 min is associated with the OPA reagent; not shown are smaller reagent peaks appearing at 15-18 min.

which exposed 100% of the sample volume to the laser flash. In Figure 1b (i), the aromatic absorbance signals of the intact caged compound **21** and the presumed aromatic nitroso keto acid side products are observed. When the detector is set at the isosbestic point for the reaction, the percent decrease in the starting material is reflected in the increase in the product peak. The reversed-phase HPLC separation in Figure 1b (i) shows the caged starting material appearing at 3.1 min, followed by elution of the side product at 7.7 min. Photolytic production of free amino acid amide was confirmed using precolumn OPA-labeling to produce the fluorescent amino acid analogues by a standard amino acid analysis protocol.[26] An HPLC trace (Figure 1b (ii)) shows that glutamine is released from **21** following a single pulse of 308-nm excimer laser light with energy of 7 mJ. The free amino group on the caged amides is also derivatized by OPA. The derivatives elute at a retention time of 12-14 min under these separation conditions (see Experimental Section). The derivatives of the caged precursors do not give a detectable fluorescence signal, but they can be observed by absorbance detection at 280 nm. Compounds **18** and **21** gave similar results. The photolysis of **17** and **20** with the α-methyl group was not as simple as that of the other derivatives, and HPLC traces showed multiple product peaks both under UV detection at 268 nm and after OPA derivatization and fluorescence detection of the products.

(26) Jones, B. N.; Pääbo, S.; Stein, S. *J. Liq. Chromatog.* **1981**, *4*, 565.

Table I. Quantum Yield Determination for the Caged Glutamine Derivatives and Comparison with *aci*-Nitro Absorbance Signals[a]

compd	concn of caged amide used (mM)	wavelength (nm)	abs[b]	quantum yield (%) (std dev)	*aci*-nitro $t_{1/2}$ (μs)
19	0.52	435	0.124	0.23 (0.09)	1800
20	0.92	420	0.068	0.13 (0.1)	360
21	1.1	435	0.120	0.24 (0.07)	720

[a] Photolysis performed in 100-mM phosphate buffer at pH 7.5 and room temperature. [b] Cuvet path length = 0.2 cm.

Table I summarizes the quantum yield of the free amino acids produced from the caged derivatives of glutamine by exposure to a single laser pulse of UV light. The table also compares the measured yields with the magnitude of the transient *aci*-nitro absorbance observed for each derivative. The photolysis conditions were chosen to convert approximately 3% of the starting material to products by a single pulse of excimer laser light at 308 nm. In order to make reliable comparisons of the transient absorbance of the different compounds shown in the table with their quantum yields, the same aliquot of caged compound used for the observation of the transient absorbance was also used for HPLC quantitation. The spectrometer alignment was adjusted so that the absorbance signal from the irradiated cuvet volume could be sampled by the detector optics. The monitored transient absorbance signal reaches a maximum at higher concentrations of caged compounds so a determination of the linearity of the signal *versus* concentration was required (see Figure 4). The data shown for compound **21** indicates significant nonlinearity of the absorbance as a function of concentration above 2 mM; it is important, therefore, to use concentrations less than 2 mM to make a valid comparison of quantum yield and *aci*-nitro absorbance. The concentration of each solution was adjusted to produce an absorbance of 0.25 through the 2-mm cuvet at 308 nm to ensure that the spatial absorbance profile for the laser light was identical in each sample. The absorbed energy was determined, both with a pyroelectric joulemeter, by measuring the difference between transmitted energies of the sample and buffer blank solutions, and with a standard ferrioxalate actinometric procedure.[27a-c] The yields of the amino acids were assayed by analytical HPLC with precolumn OPA-derivatization as detailed in the Experimental Section. The quantum yield ratios are given in Table I. A value of 0.23 for **21** is lower than the 0.8 yield found for the α-carboxyl derivative of carbamoylcholine,[13b] but higher than the 0.02 value determined for the analogous glycine derivative,[14] although the quantum yields were determined by different methods. Quantum yield determinations of the glycinamide (**15**) and γ-aminobutyramide (**16**) derivatives gave values of 0.01 and 0.18, respectively. The results in Table I suggest that for compounds **19-21** there may be a relationship between the magnitude of the *aci*-nitro intermediate absorbance and the quantum yield of released amide, although the uncertainties in the data do not permit a secure identification of such a relationship.

In the photolysis of caged ATP[28c] and of a fluorescent ATP analog,[29] the rate constant for disappearance of the

(27) (a) Kirk, A. D.; Namasivayam, C. *Anal. Chem.* **1983**, *55*, 2428. (b) Bowman, W. D.; Demas, J. N. *J. Phys. Chem.* **1976**, *80*, 2434. (c) Vincze, L.; Papp, S. *J. Photochem.* **1987**, *36*, 289.

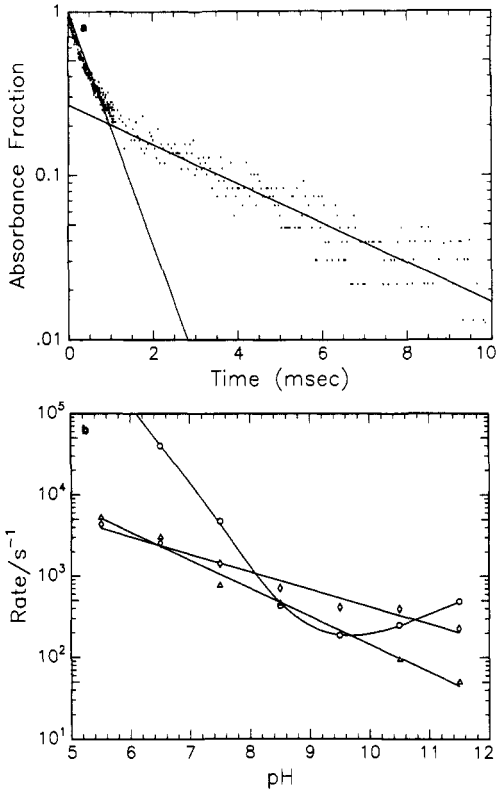

Figure 2. (a) Logarithmic plot of the *aci*-nitro intermediate absorbance decay of a 2 mM solution of **21** in 100 mM phosphate buffer, pH 7.5, monitored at 440 nm following transient excitation by a single pulse of 308-nm excimer laser light; a small permanent base line offset arising after photolysis has been subtracted before the log transformation. The solid lines are linear least-squares fits to the fast and slow parts of the data, separated at the 1-ms time point. The fraction of the fast and slow components at 440 nm are 64 and 36%, respectively, with half lives of 0.36 and 3.5 ms determined by averaging five measurements. The plotted data are simplified over the slow phase for clarity by displaying every sixteenth point of the acquired data as well as by digital noise smoothing. (b) *aci*-Nitro absorbance signal decay rates determined from the half-life values of the overall decay processes are plotted as a function of pH for compounds **19**, **20**, and **21**. Symbols represent the measured values: (○) compound **20**; (◇) compound **21**; (△) compound **19**. Buffers were all 100 mM; pH 5.5, acetate; pH 6.0, 6.5 and 7.5, phosphate; pH 8.5 and 9.5, borate; pH 10.5, bicarbonate; pH 11.5 glycine.

aci-nitro signal reflects the rate constant for formation of the desired product. The transient *aci*-nitro absorbance decay is, therefore, an important property to measure, since the rate of product formation will determine how the compounds can be used in experiments where rapid delivery of released substrates is desired. It is not known, however, whether this is a general relationship applicable to all caged compounds with different linkages.[30] Delivery of a single pulse of 308-nm radiation to **15**-**21** produced an absorbing transient (Figure 2a) with an absorbance maximum at 438 nm for **18**, **19**, and **21** (Figure 3). The band maximum was shifted to 422 nm for **17** and **20**. The width at half maximum for these bands was between 65 and 75 nm. These measurements are comparable to those

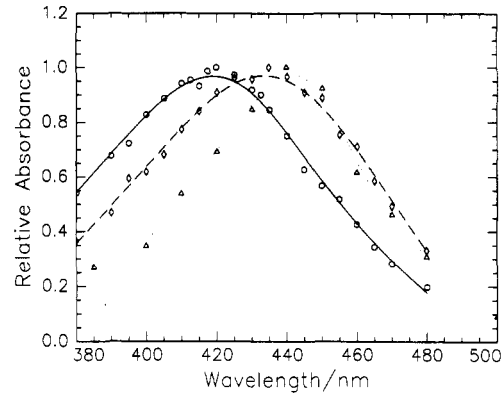

Figure 3. (a) *aci*-Nitro spectra of **19**, **20**, and **21** (glutamine analogs) at the indicated concentration in 100 mM phosphate buffer, pH 7.5: (○) compound **20**, 1.5 mM; (◇) compound **21**, 1 mM; (△) compound **19**, 0.6 mM. The absorbance measurements were normalized to the maximum observed absorbance and plotted as a fraction of the maximum.

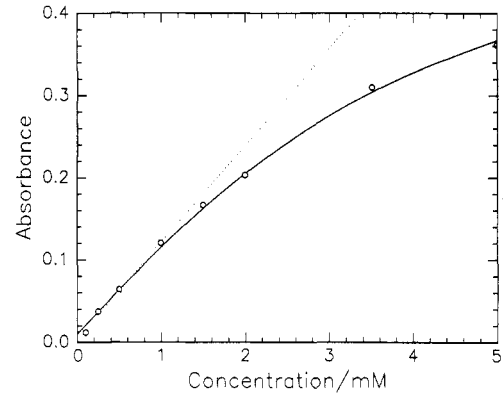

Figure 4. Saturation of transient *aci*-nitro absorbance of **21** at 440 nm as a function of concentration. Only light passing through a defined section of a 2- × 2-mm cuvet was sampled. The cross section of the sampled volume perpendicular to the laser axis was 1 × 2 mm and 1 × 1.5 mm perpendicular to the white light monitoring beam. Laser energy was 15 mJ per mm² at the front face of the cuvet.

observed for *o*-nitrotoluene,[28a] caged esters,[28b] caged phosphate ester,[28c] and caged carbamylcholine,[13b] in which the transient absorbing species is considered to be an *aci*-nitro intermediate. Figure 2a shows the semilogarithmic plot of the *aci*-nitro signal observed for **21** at pH 7.5. Nonlinear least-squares fits of this and other transient signals showed that a single exponential function is not adequate to represent the decay in all cases. Compounds **15**, **18**, **19**, and **21** produced transients similar to that in Figure 2a and are adequately represented only by a double exponential fit. In the cases where two-exponential fits were required, the absorbance amplitude of the slow phase was not more than half of the fast phase amplitude; the spectral distributions of the two phases are similar. Compounds **16**, **17**, and **20** exhibit single exponential decays of the signal over a pH range from 4 to 11, as did compound **19** below pH 7. It is important to note that if the *aci*-nitro intermediate decays to several products, the observed rate constant for its decay reflects the sum of the rate constant for the formation of these products. For these reasons, the apparent rate constants for the decay process (Figure 2b) were evaluated from the half-life value for the overall decay process. At pH 7.5 the $t_{1/2}$ values for **15** and **19** were found to be 1.8 ms, for **16**, **17**, and **20** 0.36 ms, and for **18** and **21** 0.72 ms. The $t_{1/2}$ value for the carbamate linkage[13b]

(28) (a) Wettermark, G. *J. Phys. Chem.* **1962**, *66*, 2560. Wettermark, G. *Nature* **1962**, *194*, 677. (b) Schupp, H.; Wong, W. K.; Schnabel, W. *J. Photochemistry* **1987**, *36*, 85. Zhu, Q. Q.; Schnabel, W.; Schupp, H. *J. Photochem.* **1987**, *39*, 317. (c) Walker, J. W.; Reid, G. P.; McCray, J. A.; Trentham, D. R. *J. Am. Chem. Soc.* **1988**, *110*, 7170.

(29) Wootton, J. F.; Trentham, D. R. *NATO ASI Ser. C* **1989**, *272*, 277.

(30) McCray, J. A.; Fidler-Lim, N.; Ellis-Davies, G. C. R.; Kaplan, J. H. *Biochemistry* **1992**, *31*, 8856.

Scheme II

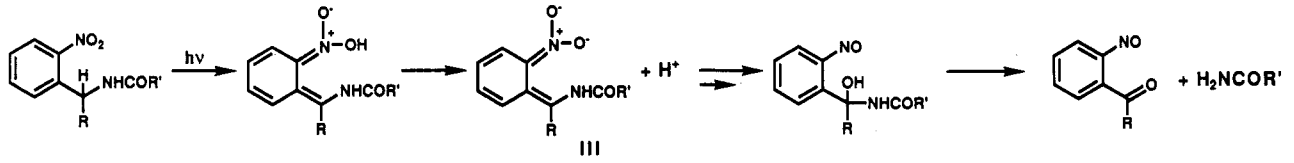

III

is 0.052 ms, for the amine linkage 1.2 ms,[14] and at pH 9.0 for the ester linkage 700 ms.[12] The effect of pH on these apparent rate constants was measured as a function of pH and found to be increased at lower pHs, as shown in Figure 2b. The pH *versus* rate profile for **17** and **20**, with a minimum at pH 9.5, is similar to the profile observed for the analogous α-methyl derivative of carbamylcholine,[13a] with a minimum at pH 8.5. The α-carboxy and benzyl derivatives show smoothly increasing rates as the pH is lowered from 11 to 4. By grouping the data according to the nature of the substituents at the α position on the precursor molecule (e.g., H, CH_3, CO_2H), it is clear that for an amide leaving group, it is the α-substituents that are the dominant structural influence on the rate–pH profile. The nature of the the amide leaving group does not appear to affect the photolysis rate. Scheme II shows the proposed photolysis mechanism[2a,25] and is consistent with the observations here of the released products (free amides and the *o*-nitrobenzoyl fragment) and the transient absorbance of the *aci*-nitro intermediate (**III**).

The time scale of the release of the amides from the photolabile *o*-nitrophenyl protecting group was unknown and has now been investigated. These studies, and the synthesis of a series of new photolabile precursors of biologically important amino acid amides, are reported here. Photolabile *o*-nitrobenzyl derivatives of amides are used in peptide synthesis to avoid rigorous acid and base conditions used in deprotection and to produce the amide group on the *N*-terminus of the peptide.[22c,31] The compounds illustrated here are suitable for preparation of amides under neutral photolysis conditions that facilitate their use in biological systems. The amide bond is formed *in situ* during the synthesis of the caged molecule, and no free amide is present until photochemically released from the *o*-nitrobenzyl group. Since the release is directed by a pulse of laser light, it is possible to spatially direct the production of the free amide. The relatively high photoproduct yield, photolysis rate under physiological pH conditions, and water solubility of compounds **15-21** make them potential candidates for sequestering a reservoir of an amino-acid amide inside a biological matrix, which can be used to provide the free amides with precise spatial and temporal control. The development of new caged substances will be useful in time-resolved experiments of catalytic mechanisms and protein:substrate interactions on the millisecond timescale that are not accessible with other techniques.

Experimental Section

Melting points were determined on a Thomas-Hoover hot-stage apparatus and are uncorrected. NMR spectra were recorded on either a Varian XL-200 (200 MHz) or a Varian XL-400 (400 MHz, ^{1}H-NMR; 100 MHz, ^{13}C-NMR); chemical shifts are expressed as parts per million (δ) downfield from tetramethylsilane or to the residual solvent signals in $CDCl_3$ at 7.24 ppm or in D_2O at 4.64 ppm. *J* values are given in Hz. Thin-layer chromatography was performed on silica gel 60F-254 precoated glass plates (layer thickness 0.25 nm, Merck) using the following solvent systems: for $\mathbf{I_a}$ and $\mathbf{II_a}$ (see Scheme I for the name of the compounds) hexane/ether (1:1) and hexane/ethyl acetate (1:1); for $\mathbf{I_b}$ and $\mathbf{II_b}$, *n*-butanol/acetic acid/water (3:1:1) and ethanol/water (9:1 + a drop of NH_4OH). The chromatograms were visualized under a UV lamp and then sprayed with ninhydrin reagent. The amide derivatives $\mathbf{I_a}$ and $\mathbf{I_b}$ were purified by vacuum liquid chromatography[32] on silica gel adsorbent (10–40 m, type-H, Sigma), using hexane as the eluent, the polarity of which was gradually increased by the addition of either ethyl acetate or ether. Elemental combustion analyses were performed by Schwarzkopf Microanalytical Laboratory Inc., Woodside, NY.

Materials. Diethyl ether was dried over sodium and distilled before use. Methylene chloride (Fisher reagent grade) was dried over CaH_2 and distilled before use. Ethyl acetate was dried over P_2O_5 and distilled. 2-Nitro-α-phenethylamine·HCl (**2**) was prepared as described previously.[13a] The following chemicals were purchased and used without further purification: 2-nitrobenzylamine·HCl (**1**) (Overlook Industries); C-(2-nitrophenyl)-glycine (Molecular Probes), *N*-t-BOC-L-aspartic acid α-*tert*-butyl ester (Chemical Dynamic Corporation), *N*-t-BOC glycine, *N*-t-BOC-γ-aminobutyric acid, and *N*-t-BOC-γ-glutamic acid-α-*tert*-butyl ester (Sigma); 1-(3-dimethylaminopropyl)-3-ethyl carbodiimide·HCl (EDCI), 4-(dimethylamino)pyridine (DMAP), *N*-hydroxybenzotriazole (NHBT), and *N*-ethylmorpholine (NEM) (Aldrich); isobutylene (Matheson). All reactions were performed under argon, unless otherwise stated.

Preparation of *C*-(2-Nitrophenyl)glycine *tert*-Butyl Ester·Monohydrochloride (3). To a mixture of *C*-(2-nitrophenyl)glycine·HCl (0.233 g, 0.1 mmol), powdered 4-Å molecular sieves (1.0 g), 1,4-dioxane (10 mL), and concentrated H_2SO_4 (0.2 mL) in a pressure bottle, precooled to −78 °C, was added isobutylene (10 mL). The bottle was stoppered and shaken in a Parr hydrogenator shaker for 2 days. The contents were filtered through a Celite pad, diluted with 50 mL of chilled water, and extracted three times with 20 mL of ethyl acetate. The organic layer was washed three times with 10 mL of saturated $NaHCO_3$ solution, once with 10 mL of H_2O, and once with 10 mL of saturated NaCl solution and then dried over anhydrous Na_2SO_4. The ester (**3**) was purified by column chromatography and isolated as its hydrochloride salt. Yield: 124 mg (43%). Mp: 128–130 °C. ^{1}H-NMR (D_2O): 8.16 (d, J = 8.15, 1H), 7.73 (t, J = 7.57, 1H), 7.64 (t, J = 8.01, 7.55, 1H), 7.50 (d, J = 7.62, 1H), 5.46 (s, 1H), and 1.26 (s, 9H). Anal. Calcd for $C_8H_8N_2O_4$·HCl: C, 49.83; H, 5.89; N, 9.67. Found: C, 50.32; H, 5.73; N, 9.66.

General Procedure for Amide Formation (8-14). To a stirred mixture of the amine·HCl **1**, **2**, or **3** (0.2 mmol), amino acid derivative **4**, **5**, **6** or **7** (0.22 mmol), EDCI (0.24 mmol), *N*-hydroxybenzotriazole (0.02 mmol), and 4-DMAP (0.02 mmol) in CH_2Cl_2 (10 mL) at 0 °C was added *N*-ethylmorpholine (0.23 mmol) dropwise during 30 min. After 12 h, and after confirming by TLC analysis that the reaction had gone to completion, the solvent was removed in a rotary evaporator, ice (~10 g) added, and the contents extracted three times with 5 mL of ethyl acetate. The combined organic layer was washed three times with 5 mL of saturated $NaHCO_3$ solution, three times with 5 mL of 10% citric acid solution, once with 5 mL of H_2O, and once with 5 mL of saturated NaCl solution and dried over anhydrous Na_2SO_4. The amide products were purified by column chromatography.[32]

(31) (a) Pillai, V. N. R. In *Organic Photochemistry*; Padwa, A., Ed.; Marcel Dekker: New York; 1987; Vol. 9, p 225. (b) Colombo, R. *Hoppe-Seyler's Z. Physiol. Chem.* **1981**, *362*, 1393.

(32) Coll, J. C.; Mitchell, S. T.; Stokic, G. J. C. *Aust. J. Chem.* **1977**, *30*, 1859.

(33) **Note Added in Proof:** Matthew, T.; Ajayaghosh, A.; Das, S.; Kamat, P. V.; George, M. V. *J. Photochem. Photobiol. A: Chemistry* **1993**, *71*, 181.

***N*-(*tert*-Butoxycarbonyl)-*N'*-(2-nitrobenzyl)glycinamide (8).** Yield: 51 mg (82%). Mp: 122–123 °C (Et_2O). ^{1}H-NMR ($CDCl_3$): 8.06 (d, J = 8.6, 1H), 7.63 (m, 2H), 7.46 (m, 1H), 6.90 (bt, 1H), 5.04 (bt, 1H), 4.70 (d, J = 6.3, 2H), 3.79 (d, J = 6.1, 2H), and 1.43 (s, 9H).

γ-[(*tert*-Butoxycarbonyl)amino)]-*N*-(2-nitro-α-methylbenzyl)butyramide (9). Yield: 60 mg (85%). Mp: 110 °C (Et_2O). ^{1}H-NMR ($CDCl_3$): 7.85 (d, J = 8.43, 1H), 7.58 (m, 2H), 7.37 (m, 1 H), 6.94 (d, J = 4.5, 2H), 5.49 (p, J = 6.99, 1H), 4.71 (bt, 1H), 3.13 (q, J = 6.35, 2H), 2.20 (t, J = 6.97, 2H), 1.74 (m, 2H), 1.56 (d, J = 7.02, 3H), and 1.45 (s, 9H).

***N*-(*tert*-Butoxycarbonyl)-*N'*-(2-nitro-α-methylbenzyl)-L-asparagine α-*tert*-Butyl Ester (10).** Yield: 65 mg (74%) yellow gum. ^{1}H-NMR ($CDCl_3$): 7.89 (t, J = 6.68, 1H), 7.56 (m, 1H), 7.48 (d, J = 7.82, 1H), 7.39 (m, 1H), 6.5 (bm, 1H), 5.64 (bm, 1H), 5.49 (m, 1H), 4.69 (bd, 1H), 2.70 (m, 2H), 1.53 (d, J = 7.0, 3H), 1.44 (s, 9H), and 1.43 (s, 9H).

***N*-(*tert*-Butoxycarbonyl)-*N'*-(2-nitro-α-(*tert*-butoxycarbonyl)benzyl-L-asparagine α-*tert*-Butyl Ester (11).** Yield: 94 mg (90%), yellow gum. ^{1}H-NMR ($CDCl_3$): 8.05 (d, J = 8.57, 1H), 7.59 (m, 2H), 7.5 (m, 1H), 6.84 (dd, 1H), 5.96 (t, J = 7.23, 1H), [5.72 (d), 5.32 (d) = 1H], 4.38 (m, 1H), 2.78 (m, 2H), 1.36 (s, 9H), and 1.35 (s, 9H).

***N*-(*tert*-Butoxycarbonyl)-*N'*-(2-nitrobenzyl)-L-glutamine α-*tert*-Butyl Ester (12).** Yield: 94 mg (97%), yellow gum. ^{1}H-NMR ($CDCl_3$): 8.06 (d, J = 8.3, 1H), 7.66 (d, J = 7.73, 1H), 7.61 (t, J = 7.28, 1H), 7.45 (t, J = 7.46, 1H), 6.87 (bt, 1H), 5.20 (d, J = 8.0, 1H), 4.69 (d, J = 6.16, 2H), 4.13 (m, 1H), 2.29 (m, 2H), 2.17 (m, 1H), 1.85 (m, 1H), 1.45 (s, 9H), and 1.42 (s, 9H). ^{13}C-NMR ($CDCl_3$): 218.05, 173.26, 173.21, 157.64, 135.41, 133.87, 129.89, 126.09, 61.84, 54.63, 42.25, 33.92, 30.75, 29.52 and 29.27.

***N*-(*tert*-Butoxycarbonyl)-*N'*-(2-nitro-α-methylbenzyl)-L-glutamine α-*tert*-Butyl Ester (13).** Yield: 88 mg (98%), yellow gum. ^{1}H-NMR ($CDCl_3$): 7.87 (dd, J = 6.96, 1.77, 1H), 7.56 (m, 2H), 7.38 (t, J = 6.59, 1H), 7.16 (bd, J = 4.2, 1H), 7.04 (bd, J = 4.2, 1H), 5.50 (m, 1H), 5.24 (t, J = 7.82, 1H), 2.26 (m, 3H), 1.78 (m, 1H), 1.58 and 1.57 (2d's, J = 6.89, 3H), 1.47 and 1.46 (m, 18H). ^{13}C-NMR ($CDCl_3$): 172.60, 172.53, 158.30, 157.45, 134.57, 129.48, 129.08, 125.96, 54.6, 54.5, 47.44, 33.83, 31.16, 31.03, 27.61, 29.23, 23.01, and 22.9.

***N*-(*tert*-Butoxycarbonyl)-*N'*-(2-Nitro-α-(*tert*-butoxycarbonyl)benzyl-L-glutamine α-*tert*-Butyl Ester (14).** Yield: 105 mg (98%), yellow gum. ^{1}H-NMR ($CDCl_3$): 8.07 and 8.03 (dd, J = 7.89, 1.2, 1H), 7.62 (d, J = 4.2, 2H), 7.49 (m, 1H), [7.25 (bd), 6.95 (bd) = 1H], 6.03 (m, 1H). 5.18 (m, 1H), 4.2 (m, 1H), 2.31 (m, 3H), 1.96 (m, 1H), and [1.44, 1.42, 1.41, 1.37, and 1.35 (s, 18H)].

General Procedure for the Deprotection of *N*-t-BOC and t-BOC. (i) Preparation of 15–17, 19, and 20 from 8–10, 12, and 13. To a stirred solution of the amide (0.1 mmol) in ethyl acetate (1 mL), cooled to –78 °C, was introduced a saturated solution of anhydrous HCl in ethyl acetate (1 mL) and the stirring continued for 12 h at room temperature (the disappearance of the starting material was checked by TLC analysis). The solvent was removed in a rotary evaporator, and the product was crystallized from ethylacetate-ether.

***N*-(2-Nitrobenzyl)glycinamide·HCl (15).** Yield: 22 mg (98%). Mp: 196–199 °C. ^{1}H-NMR (D_2O): 7.97 (d, J = 8.25, 1H), 7.50 (m, 3H), 4.61 (s, 2H), 3.7 (s, 2H). Anal. Calcd for $C_9H_{11}N_3O_3$·HCl: C, 43.9; H, 4.88, 17.07. Found: C, 44.01; H, 4.73; N, 16.91.

***N*-(2-Nitro-α-methylbenzyl)-γ-aminobutyramide·HCl (16).** Yield: 76 mg (93%). Mp: 179–190 °C. ^{1}H-NMR (D_2O): 7.79 (d, J = 8.3, 1H), 7.50 (m, 2H), 7.36 (m, 1H), 5.19 (q, J = 6.59, 1H), 2.82 (m, 2H), 2.22 (m, 2H), 1.74 (m, 2H) and 1.40 (d, J = 6.98, 3H). Anal. Calcd for $C_{12}H_{17}N_3O_3$·HCl: C, 50.0; H, 6.25; N, 14.58. Found: C, 49.94; H, 6.19; N, 14.4.

***N*-(2-Nitro-α-methylbenzyl)-L-asparagine·HCl (17).** Yield: 31 mg (97%). Mp: 180 °C dec. ^{1}H-NMR (D_2O): 7.75 (d, J = 8.22, 1H), 7.51 (t, J = 7.38, 1H), 7.42 (t, J = 8.11, 1H), 7.30 (t, J = 7.46, 1H), 6.19 (t, J = 1.29, 1H), 5.16 (q, J = 6.84, 1H), 4.03 (m, 1H), 2.77 (m, 2H), 1.33 (4 line, J = 7.83 and 6.90, 3H). Anal. Calcd for $C_{12}H_{15}N_3O_5$·HCl: C, 45.28; H, 5.03; N, 13.2. Found: C, 46.95; H, 4.99; N, 12.33.

***N*-(2-Nitrobenzyl)-L-glutamine·HCl (19).** Yield: 31 mg (98%). Mp: 160 °C dec. ^{1}H-NMR (D_2O): 7.87 (d, J = 8.0, 1 H), 7.49 (t, J = 7.57, 1H), 7.32 (m, 2H), 6.18 (two line, 1H), 4.47 (dd, 2H), 3.83 (t, J = 6.23, 1H), 2.33 (m, 2H), and 2.01 (m, 2H). ^{13}C-NMR (D_2O); 177.04, 174.38, 150.3, 136.97, 135.3, 134.01, 132.78, 131.41, 127.87, 54.99, 43.44, 33.64, and 28.32. Anal. Calcd for $C_{12}H_{15}N_3O_5$·HCl: C, 45.28; H, 5.03; N, 13.2. Found: C, 47.03; H, 5.07; N, 13.09.

***N*-(2-Nitro-α-methylbenzyl)-L-glutamine·HCl (20).** Yield: 32 mg (97%). Mp: 185 °C dec. ^{1}H-NMR (D_2O): 7.73 (d, J = 8.27, 1H), 7.50 (t, J = 7.33, 1H), 7.43 (t, J = 4.58, 1H), 7.30 (t, J = 7.56, 1H), 5.31 (q, J = 6.95, 1H), [3.78 (t, J = 4.1) and 3.7 (t, J = 4.1) 1H], 2.27 (m, 2H), 1.93 (m, 2H) and 1.33 (d, J = 7.03, 3H). ^{13}C-NMR (D_2O); 183.2, 181.58, 157.68, 147.94, 143.74, 137.99, 137.0, 134.15, 75.72, 62.11, 40.47, 35.27 and 29.85. Anal. Calcd for $C_{13}H_{17}N_3O_5$·HCl: C, 46.99; H, 5.42; N, 12.65. Found: C, 47.31; H, 5.43; N, 12.35.

(ii) Preparation of 18 and 21 from 11 and 14. Trifluoroacetic acid (0.3 mL) was added to the amide (0.1 mmol) at 0 °C, stirred for 20 h at room temperature, and cooled to –78 °C, and ether (4 mL) was added. The precipitated solid was filtered, washed with CH_2Cl_2, and dried.

***N*-(2-Nitro-α-carboxybenzyl)-L-asparagine·CF_3CO_2H (18).** Yield: 35 mg (82%). Mp: 165–168 °C dec. ^{1}H-NMR (D_2O): 7.97 (d, J = 9.02, 1H), 7.59 (t, J = 7.66, 1H), 7.44 (t, J = 7.55, 2H), 5.83 (s) and 5.82 (s) 1H, 3.98 (m, 1H), 2.89 (m, 2H). ^{13}C-NMR (D_2O): 175.36, 174.11, 173.83, 172.83, 172.74, 149.22, 136.78, 133.75, 133.65, 133.48, 131.85, 127.6, 57.65, 57.56, 52.36, 52.30, 36.84 and 36.38. Anal. Calcd for $C_{12}H_{13}N_3O_7$·CF_3CO_2H: C, 39.53; H, 3.29; N, 9.88. Found: C, 38.9; H, 3.43; N, 9.71.

***N*-(2-Nitro-α-carboxybenzyl)-L-glutamine·CF_3CO_2H (21).** Yield: 31 mg (70%). Mp: 160–165 °C dec. ^{1}H-NMR (D_2O) 7.97 (d, J = 8.57, 1H), 7.60 (t, J = 7.55, 1H), 7.45 (m, 2H), [5.853 and 5.849 (1H)], 3.72 (q, J = 6.42, 1H), 2.38 (m, 2H) and 1.99 (m, 2H). ^{13}C-NMR (D_2O): 179.18, 179.10, 178.22, 178.17, 177.61, 177.55, 152.34, 139.92, 136.65, 136.53, 135.09, 130.75, 60.38, 58.09, 57.95, 36.10, 35.87, 30.87, and 30.81. Anal. Calcd for $C_{13}H_{15}N_3O_7$·CF_3CO_2H: C, 41.0; H, 3.64; N, 9.57. Found: C, 39.68; H, 3.76; N, 9.41.

Laser-Flash Photolysis. Radiation at 308 nm from a Lumonics TE861M XeCl excimer laser was focused to irradiate a volume of 8 mm^3 of a 2- × 2-mm quartz cuvet. The pulse energy was between 10 and 50 mJ delivered in 10–20-ns pulses; flux densities of 1–8 mJ per mm^2 were produced at the front face of the cuvet. The transient absorbance of intermediates produced during photolysis was observed at right angles to the laser irradiation by passing a collimated beam of light from a stabilized quartz tungsten halogen source through a Corning WGS360 cutoff filter and then through the cuvet oriented with faces perpendicular to the irradiation and monitoring beams. The white light beam itself produced negligible photolysis or heating of the sample, as determined by monitoring over time both the solution absorbance at the wavelength of maximum starting material absorbance and the temperature with an inserted thermocouple with a 0.1 °C sensitivity. For detection of the *aci*-nitro intermediate, the image of the irradiated cuvet volume closest to the laser was magnified 6.5 times and focused on to the 250-μm entrance slit of a 0.3-m single-pass monochrometer, and the spectral distribution of the transmitted light was measured at selected wavelengths over the range 350–500 nm. Light from the monochrometer was detected with a photomultiplier (Thorn EMI 9635QB), the photocurrent was converted to voltage, amplified, and filtered at four times the data acquisition rate, and signal transients were either photographed and manually digitized from an analog oscilloscope trace or digitized into a personal computer for storage. The data collection time was determined by the decay rate of the signal for each compound and was at least six times the value of the time constant of the slowest component observed in the signal to ensure adequate representation of the decay for subsequent fitting operations. The transient absorbance signals were fitted to one- or two-exponential decays using the nonlinear least-squares analysis program Genplot (Computer Graphics, Ithaca, NY).

Photolysis Product Spectra. Solutions of compounds 15-21 at concentrations of 0.5-2 mM in 200 mM HEPES buffer at pH 7.4 were photolyzed by single flashes of 8-20 mJ UV light at 308 nm from the excimer laser. The photolysis was performed on 30 μL of solution in a 2- × 2-mm quartz cuvet, which was

transferred to the spectrophotometer immediately after each laser pulse for measurement of the absorption spectrum.

Chromatography. Analytical HPLC was performed on a Waters 600E instrument using a Waters μBondapak C-18 300- × 4.5-mm reversed-phase column. Phthaldialdehye labeling was used to produce fluorescent derivatives of free amino acids.[26] A 20-μL aliquot of photolyzed solution (0.5-2 mM in 100 mM phosphate buffer, pH 7.5) was diluted to 50 μL and allowed to react with an equal volume of OPA reagent (Sigma) for 60 s. Twenty μL of the mixture was injected on the column, running with isocratic elution at 1.5 mL/min of 30% methanol/70% 50 mM phosphate buffer, pH 6.3. The peaks were recorded with an ISCO FL-2 fluorescence detector (350-nm excitation and 430-nm detection band filters) and quantified with a chromatographic integrator. Underivatized samples were separated on the same column using 1.5 mL/min isocratic elution with 5% methanol/95% 50 mM phosphate buffer, pH 3.0, as the running buffer. A Waters 486 UV–vis detector was used in this case.

Acknowledgment. This work was supported by a grant (GM04842) awarded to G.P.H. by the National Institutes of Health. R.W. was supported by NIH training grant T32 GM08267-04. We thank Dr. Gerald Feigenson for the use of his spectrophotomer, Susan Coombs for her invaluable editorial assistance, and Lisa Miller for preparing the manuscript.